Testing the noble gas paleothermometer with a yearlong study of groundwater noble gases in an instrumented monitoring well

Chris M. Hall,[1] M. Clara Castro,[1] Kyger C. Lohmann,[1] and Tie Sun[1,2]

Received 20 May 2011; revised 27 February 2012; accepted 7 March 2012; published 17 April 2012.

[1] We report the results of a yearlong noble gas study conducted in 2008–2009 together with continuous physical and chemical measurements collected in a monitoring well in an aquifer in southern Michigan. Conditions near the water table are correlated with noble gas concentrations, corresponding noble gas temperatures (NGTs), and precipitation events. This yearlong study is the first noble gas field test that has employed natural recharge and in situ monitored conditions, with minimal disturbance of the unsaturated zone. This detailed study demonstrates that significant changes in conditions near the water table can occur over a year that can greatly affect NGTs. Results show that precipitation events are detected within hours at the water table, but a lag in pressure response argues for a long time constant for gas transport within the unsaturated zone. There is strong evidence for the depletion of oxygen near the water table, which affects the noble gas air-saturated water component. During reducing conditions there is evidence for significant noble gas degassing. Rain from the passage of Hurricane Ike caused a significant shift in stable isotope ratios and injection of a large quantity of excess air and likely led to a much more oxygen-rich environment in the soil gas. Although individual models can account for NGTs over portions of the record, no single NGT model can account for all features observed over the entire study. It is likely that the NGT temperature proxy must be viewed as an average of recharge conditions over several years.

Citation: Hall, C. M., M. C. Castro, K. C. Lohmann, and T. Sun (2012), Testing the noble gas paleothermometer with a yearlong study of groundwater noble gases in an instrumented monitoring well, *Water Resour. Res.*, *48*, W04517, doi:10.1029/2011WR010951.

1. Introduction

[2] The noble gas temperature (NGT) proxy has been used for nearly four decades [*Mazor*, 1972] as an indicator of past climate. It utilizes the known temperature dependence of the solubility of the four heaviest stable noble gases (Ne, Ar, Kr, and Xe), with the heavier noble gases being more temperature sensitive than the lighter ones [*Ozima and Podosek*, 2006]. In practice, the concentrations of the atmospheric component of the heavier stable noble gases (^{20}Ne, ^{36}Ar, ^{84}Kr, and typically ^{132}Xe) in groundwater are assumed to be a simple function of conditions existing at the water table at the time of recharge. This contrasts with tritiogenic, radiogenic and mantle-derived components, which can significantly build up over time. Because the air-saturated water (ASW) component is conservative and dispersion of this component within an aquifer is a very slow process [e.g., *Stute and Schlosser*, 1993; *Castro et al.*, 2007], groundwater is expected to record the temperature of the ground air in the recharge zone. Ground air temperature at the water table is commonly assumed to be that of the mean annual air temperature (MAAT) within $\pm 1^{\circ}$C [see, e.g., *Stute and Schlosser*, 1993; *Kipfer et al.*, 2000]. NGTs have commonly been used to reconstruct continental temperatures over the past few tens of thousands of years [e.g., *Stute and Deak*, 1989; *Stute et al.*, 1992, 1995; *Aeschbach-Hertig et al.*, 2002a; *Castro and Goblet*, 2003; *Beyerle et al.*, 2003; *Ma et al.*, 2004; *Castro et al.*, 2007], with particular attention being paid to the contrast in temperatures between the current climate and that during the Last Glacial Maximum (LGM), which is a critical test for general circulation models.

[3] Early on, it was noted that noble gas concentrations in groundwater, especially those of the lighter noble gases, exceeded levels expected for ASW. *Heaton and Vogel* [1981] attributed these anomalously high noble gas concentrations to the incorporation and dissolution of air bubbles associated with rapid water table level changes. This excess air (EA) component is not a direct measure of temperature, rather it reflects the air composition in the dissolved bubbles. It should be noted that the EA component is richer in the light gases, especially Ne, than is the ASW component. The simplest NGT model, often referred to as the unfractionated air (UA) model assumes that the EA component consists of noble gases whose relative concentrations match those of standard air [*Stute and Schlosser*, 1993]. In practice with the UA model, two parameters (temperature and the size of the EA component) are adjusted to find an optimal fit to the measured noble gas data. However, the

[1]Department of Earth and Environmental Sciences, University of Michigan, Ann Arbor, Michigan, USA.
[2]Now at Center for Petroleum and Geosystems Engineering, Cockrell School of Engineering, University of Texas at Austin, Austin, Texas, USA.

0043-1397/12/2011WR010951

unfractionated air EA component does not always adequately model measured noble gas concentrations in groundwater [e.g., *Stute et al.*, 1995], which has led to the development of a series of alternative models for the EA component [see, e.g., *Aeschbach-Hertig et al.*, 2008].

[4] Temperature and EA estimation was improved dramatically by the employment of nonlinear inverse techniques, thereby allowing rigorous statistical tests to determine the adequacy of competing NGT models [*Ballentine and Hall*, 1999; *Aeschbach-Hertig et al.*, 1999]. Armed with these mathematical tools, it has been possible to explore the numerical properties of a variety of models with alternative versions of both the EA [e.g., *Aeschbach-Hertig et al.*, 2000; *Sun et al.*, 2008] and the ASW components [*Mercury et al.*, 2004; *Hall et al.*, 2005; *Castro et al.*, 2007]. An overall review of the statistical properties of a wide variety of NGT models is provided by *Sun et al.* [2010].

[5] In recent years, in addition to field experiments [e.g., *Clark et al.*, 2005; *Clark*, 2007; *Klump et al.*, 2007; *Cey et al.*, 2008] a number of laboratory tests of mechanisms for the acquisition of the ASW and EA components at the water table [e.g., *Holocher et al.*, 2002; *Aeschbach-Hertig et al.*, 2008] were conducted. Control of variables in laboratory experiments was employed in order to simplify the process of interpretation. In the case of the field experiments, artificial recharge was used and in the *Klump et al.* [2007] study, trenches were dug into the unsaturated zone to monitor the uptake of noble gases as recharge water moved toward the water table. Both field and laboratory experiments previously conducted have thus led to disturbed or artificial conditions and, possibly to oversimplifications. Here, for the first time, we present the results of a yearlong groundwater noble gas study conducted in situ, under barely disturbed conditions in which, in addition to noble gases, continuous measurements of physical and chemical processes were made that could be correlated with natural recharge from precipitation. The present study was carried out in the upper portion of the unconfined Glacial Drift aquifer in SE Michigan, in the monitoring well originally presented by *Sun et al.* [2008]. The results here presented shed light on factors that control noble gas concentrations in groundwater in the field, under as natural a set of conditions as could be reasonably achieved. Our results demonstrate that complex physical and chemical changes that are driven by sudden meteorological events can have significant effects on noble gas concentrations in groundwater on the time scale of days, weeks and months, and suggest that the NGT paleothermometer must average conditions over an extended period of time, possibly several years, in order to yield meaningful temperature estimates.

2. Methods

2.1. Sonde Deployment and Hydrogeological Setting

[6] This study was conducted in a 5 cm diameter monitoring well located at 42°18.496′N, 83°45.982′W in the unconfined upper aquifer of the Glacial Drift Aquifer in Ann Arbor, Michigan (Figure 1). The aquifer, with a saturated thickness of ~11.2 m consists of unconsolidated sand and is bounded by a massive clay layer at the bottom. The unsaturated zone is ~13.2 m thick and consists of an intercalation of gravel and sand layers as described in the auxiliary material of *Sun et al.* [2008]. The monitoring well has a total depth of 24.38 m and is screened over the lower 12.19 m [cf. *Sun et al.*, 2008], i.e., over the entire saturated portion of the aquifer. The well was screened over the entire thickness of the aquifer to ensure that natural conditions with respect to water flow remain as undisturbed as possible, in addition to reproducing sampling conditions of typical noble gas studies. This allows for the comparison of our results with previous studies. A well that is screened throughout the entire saturated thickness of the aquifer results in some vertical mixing during noble gas sampling. However, as discussed in detail by *Sun et al.* [2008], mixing is restricted to a small vertical region near the pump.

[7] Our study site is located on the northern side of a hill whose peak lies ~18 m above, in an extended plateau (Figure 1). In the vicinity of our well, water flows downward toward the Huron River with a NNE direction under a hydraulic gradient of 0.025. Horizontal and vertical hydraulic conductivities estimated in the upper aquifer at a site nearby are $\sim 5.3 \times 10^{-4}$ m s^{-1} (model B [*Cypher and Lemke*, 2009]), leading to a pore velocity of 3.8×10^{-5} m s^{-1} (3.3 m d^{-1}) for a porosity of 35%, a value typical of unconsolidated sand [e.g., *Freeze and Cherry*, 1979]. If one takes these values as representative of the average hydraulic conductivity in and around our study area, this implies that any changes of noble gas composition and other measured parameters observed within hours or a few days of a rainfall episode are mostly the result of local recharge rather than mixing with water recharged at other locations. It is possible, however, that some degree of mixing might occur. Horizontal and vertical hydraulic conductivities might present some spatial variation in the area (e.g., model C [*Cypher and Lemke*, 2009]). Such variability might lead to horizontal and vertical hydraulic conductivity values as high as $\sim 9 \times 10^{-4}$ m s^{-1}, corresponding to a pore velocity of 6.4×10^{-4} m s^{-1} (5.5 m d^{-1}). In anisotropic media, horizontal and vertical hydraulic conductivities down to $\sim 9 \times 10^{-5}$ m s^{-1} (horizontal pore velocity of 6.4×10^{-6} m s^{-1} or 0.6 m d^{-1}) and $\sim 9 \times 10^{-6}$ m s^{-1} (vertical pore velocities of 6.4×10^{-7} m s^{-1} or 0.06 m d^{-1}), respectively, might be observed. However, such values are likely to be extremes.

[8] The average recharge rate of the Glacial Drift Aquifer in Michigan is estimated to be 214 mm yr^{-1}, reaching values up to 566 mm yr^{-1} where only coarse textural material is present [*Rutledge*, 1993; *Holtschlag*, 1996, 1997; *Hoaglund et al.*, 2002].

[9] A YSI model 600XLM sonde, equipped with a model 6562 dissolved oxygen (DO) sensor, was deployed in the well on 29 March 2008. All times in plots for this study are relative to days after 29 March 2008. The sensor was calibrated to 100% O_2 saturation using water-saturated air prior to insertion into the well. The sonde was programmed to automatically measure DO, water depth, water temperature, salinity, pH and oxidation reduction potential (ORP) every 15 min. At the time of the deployment, a Proactive model P-10330 12V DC pump was placed 0.656 m below the sonde's sensors so that water sampling could be performed while the sonde remained in place. Typically, when water was sampled for noble gas analysis, data was offloaded from the sonde using an RS-232 data link. The

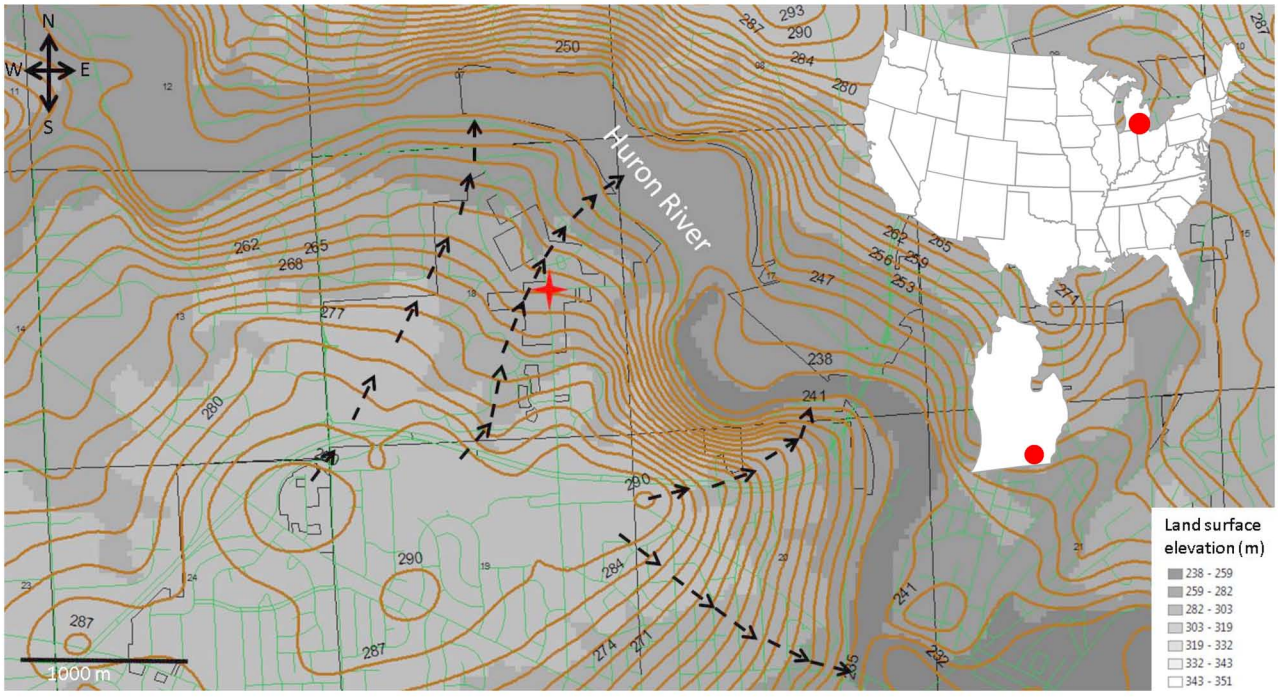

Figure 1. Location map showing the study area. The location of the study area within the 48 contiguous states of the United States is shown in the inset map in the top right (red circle), and below that the study area within the lower peninsula of the state of Michigan is also indicated. The location of the monitoring well is indicated by a red cross. Surface topography is shown as shades of gray together with equipotential lines shown as brown contours (labeled in meters). The direction of groundwater flow is indicated by dashed black lines. GIS data used to construct the map are from the Michigan State Geographic data library (http://www.mcgi.state.mi.us/mgdl/).

initial water table depth was 13.18 m from the surface, which was 0.99 m below the top of the well screen.

[10] Water depth data collected refers to the position of the cluster of sonde sensors relative to the water table. The sonde was held at a fixed position relative to the surface and therefore an increase in water depth at the position of the sensor corresponds to an equal rise in the water table level. Water samples were from the water inlet of the pump that was 0.656 m below the sensors. As noted by *Sun et al.* [2008], there is an effective vertical mixing within the well casing. A simple flow model was developed to estimate the effective mid point water depth of a pumped water sample (see *Sun et al.* [2008, auxiliary material] for details). With a typical pump depth of roughly 1.5–2 m, a pumping rate of 4 L min^{-1} and a sampling duration of about 10 min, we estimate the effective mean depth of the water retrieved for noble gas analysis to be approximately 3.5 m.

[11] The sonde remained undisturbed until day 57 of the experiment (25 May 2008) when it was noticed that the depth of the sensors below the water table was approaching 1 m and it was feared that water might damage some electrical connections above the sonde and therefore the sonde was raised 0.374 m. On day 154 (30 August 2008), the sonde was removed from the well and repositioned because the water table had dropped to the point where it was feared that the sonde sensors soon might no longer be immersed in water. On that day, it was noticed that the DO sensor could no longer be calibrated to water-saturated air. Therefore, the DO sensor's membrane was replaced and the sensor was recalibrated. Following the membrane replacement, the sonde was redeployed into the well, but at a depth 0.374 m below its previous depth. We estimate that the DO data is likely only to be reliable for ~20–30 days after the initial deployment and for a similar period after the membrane replacement. The water depth record has been corrected accordingly by removing the offsets created on days 57 and 154 so that a continuous record of water table depth variation could be deduced. However, the offsets do affect the other measured parameters, especially ORP, and this should be taken into account when interpreting results from the sensors near the times of the sonde relocations.

[12] It should be noted that all sensors were calibrated before deployment, but the DO sensor was the only sensor that was recalibrated during the deployment. This means that calibration drift might affect the absolute accuracy of some parameter readings, but it was decided that the highest priority was to acquire continuous data. Indeed, the absolute accuracy of the measurements is much less important in this study than detecting relative changes. On the other hand, conductivity (i.e., salinity) and depth can retain accurate readings for many months, and temperature readings cannot be recalibrated in the field (Gary Lorden at YSI, personal communication, 2011). In addition, the remarkable correlation observed between water depth and barometric pressure as shown below clearly indicates that water table variations were being properly measured by the

sonde, an observation consistent with information provided to us by YSI. The main focus of the experiment was to be able to detect sampling artifacts and the effects of recharge from precipitation events. All sensors responded to both sampling and precipitation throughout the duration of the experiment and slow calibration drift would not invalidate the response time lags seen in the sonde data. In addition, recalibration would have introduced discontinuities within the sensor records that would make interpretation more difficult.

[13] Meteorological data was collected from the NOAA national climate data center (http://cdo.ncdc.noaa.gov/qclcd/QCLCD?prior=N) for the weather station at the Ann Arbor Municipal Airport (AAMA) so that changes within the well could be correlated with meteorological events. The AAMA data are based on local standard time while the sonde's clock was set to daylight savings time. Sonde data were time shifted by 1 h to match the times for the AAMA data. In addition, to perform data analysis for the two data sets, it was convenient to standardize the measurement times to the same values. Thus, AAMA measurement times were used as the standard, and sonde data were linearly interpolated to AAMA times using the R approx function.

[14] It was noticed that AAMA measured atmospheric pressure had a significant degree of correlation with the sonde depth data (Figure 2). The 600XLM sonde is equipped with a pressure compensation system that uses an air tube running from the water depth sensor to the surface that eliminates the effect of varying atmospheric pressure upon the pressure sensor that is used to estimate water depth. Despite this compensation system, depth could be seen to move in concert with changes in atmospheric pressure and the sense of the correlation is opposite to the effect one would see if the compensation system was not working correctly. The correlation coefficient between water depth and variations of atmospheric pressure about the mean was –0.2508. An air pressure increase can immediately be felt in the center of the well, and if such a pressure increase propagated instantly through the $\sim$13 m of sediment in the unsaturated zone, no change in water depth would occur. However, if the increase in air pressure away from the well takes much longer to reach the vicinity of the water table, there will be a drop in the water level within the well (i.e., a decrease in the depth reading). In other words, an increase in air pressure will push water out of the well casing into the surrounding saturated zone until the pressure imbalance in the unsaturated zone can be restored.

[15] This barometric effect on water head was quantitatively investigated by *Rasmussen and Crawford* [1997], who set out a method for fitting a pressure response function to water head data using barometric pressure. The instantaneous response, or barometric efficiency is defined as $\alpha = -\Delta W/\Delta B$, where W and B are the water head and barometric pressure, respectively. The complete pressure response is defined as a series of α values as a function of the time lag from an instantaneous unit step function change in pressure. *Toll and Rasmussen* [2007] describe a software package called BETCO that fits a step function response water to head data taking both barometric pressure and earth tide effects into account. Synthetic earth tide data for the duration of the field experiment at the well site were calculated using the TSOFT program [*Van Camp and Vauterin*, 2005] and this was combined with AAMA barometric pressure data as input into the BETCO program with

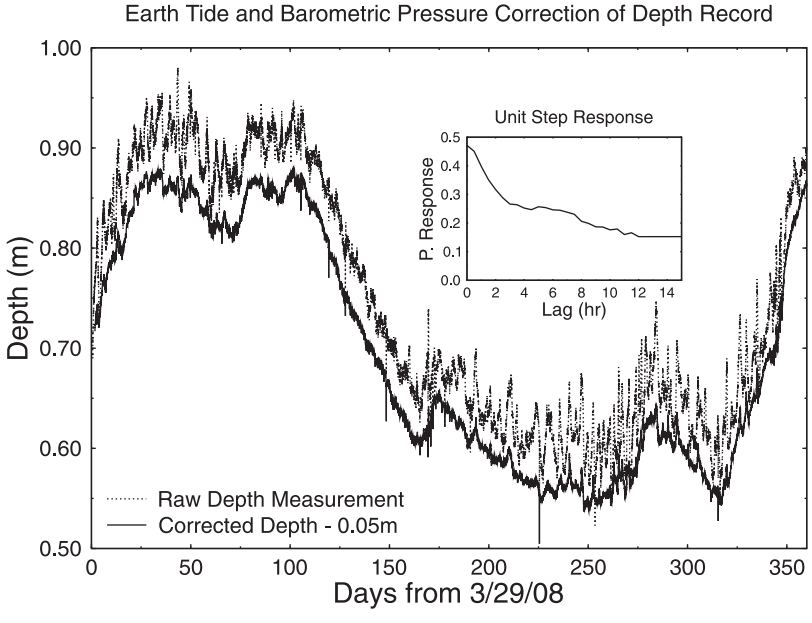

Figure 2. Raw water depth as measured by the sonde pressure sensor (dashed line) and corrected depth record offset down by 0.05 m for clarity (solid line). The corrected record was fit by the BETCO program [*Toll and Rasmussen*, 2007] using a 24 h maximum lag response function. Barometric pressure was from the Ann Arbor Municipal Airport (AAMA) meteorological record, and synthetic Earth tide data were estimated for the well site using the TSOFT program [*Van Camp and Vauterin*, 2005]. The inset shows the unit response function produced by the BETCO program.

a maximum lag time of 24 h. The results of this fit are shown in Figure 2, with both the raw and corrected water depth records plotted (the latter offset down by 0.05 m for clarity). The inset in Figure 2 shows the step function response for this site and the barometric efficiency at zero lag (i.e., $\alpha(0)$) is 47%. It is possible that the ~1–1.5 m of open screen above the water table provides a shortened pathway for air to enter the unsaturated zone near the water table, which would have the effect of muting the air pressure response within the well and thereby reducing the initial barometric efficiency.

[16] The step function response is typical for those shown by *Rasmussen and Crawford* [1997] for unconfined aquifers. However, it should be noted that the step response function is essentially flat from 12 h to the maximum assumed lag of 24 h. This suggests that there is a long-term delay in the pressure response of the unsaturated zone to changes in atmospheric pressure. Figure 2 also shows that the *Toll and Rasmussen* [2007] algorithm is very successful in removing most of the high-frequency noise seen in the water depth record.

[17] A portable CO_2 sensor was also initially deployed with the sonde and pump stack, but contact with groundwater damaged the sensor and no useable data from it was obtained. However, *Sun et al.* [2008] reported measured CO_2 concentrations in air within the well near the water table on five dates from 14 July to 7 October 2007. The concentrations dropped from a high of 1.56% in summer to a low of 0.16% in the fall. Over this same period, the dissolved oxygen concentration in water at the water table ranged from 25.6% to 43.7%, which corresponds to an O_2 concentration in air that ranges from 5.4% to 9.2%. Using the measured dissolved oxygen to estimate pO_2 in soil gas near the water table and adding this to the CO_2 concentrations, the sum of O_2 and CO_2 in air near the water table ranged from 6.1% to 10.0%. Given that free air has an O_2 concentration of 21%, the apparent drop in the partial pressure of O_2 at the water table is not completely compensated for by an equivalent rise in CO_2 concentration, and *Sun et al.* [2008] suggested that this was due to the high solubility of CO_2 in water.

2.2. Oxygen Isotopic Analysis

[18] Oxygen isotopic determination of water was performed at the University of Michigan Stable Isotope Laboratory using continuous flow via a Thermo Finnigan Gas Bench II coupled to the inlet of a Thermo Finnigan Delta V Plus mass spectrometer. Half a milliliter of water per sample or standard was injected into a preevacuated Labco exetainer and loaded into the Finnigan Gas Bench II sample tray. A CTC Analytics PAL Autosampler flushed samples with a 0.3% CO_2 in He mixture for 8 min each, and samples were allowed to equilibrate for two days at 30°C.

[19] Samples were then flushed with pure He for 8 min, with the sample gas being carried via He flow and cleaned of water via the Gas Bench water traps, and fed through a GC column maintained at 70°C. The gas was then admitted through a capillary to the inlet of the mass spectrometer where multiple sample peaks were measured against the CO_2 reference gas peaks. Data are normalized and reported relative to the VSMOW/VSLAP scale, and accuracy and precision are ±0.1‰.

2.3. Hydrogen Isotopic Analysis

[20] Deuterium isotopic analysis of water was performed at the University of Michigan Stable Isotope Laboratory using continuous flow via a Thermo Finnigan High Temperature Conversion Elemental Analyzer (TC/EA Device) coupled to the inlet of a Finnigan Delta V Plus mass spectrometer through a Thermo Finnigan ConFlo IV interface [*Gehre et al.*, 2004]. Water samples were loaded into vials and sealed with Teflon septa. A CTC Analytics PAL autosampler was used to clean the syringe between samples and inject the sample into the TC/EA reactor that had been packed with a glassy carbon reactor and glassy carbon granulate. A 400 nanoliter sample of water was injected and the reaction temperature was 1400°C. The hydrogen in the water is converted to H_2 by pyrolysis and the oxygen was converted to CO. The gases were separated in the TC/EA by an isothermal gas chromatograph, and admitted to the Delta V Plus IRMS via a Thermo Finnigan ConFlo IV interface. Sample peaks were measured against reference gas of known composition, and data are normalized and reported on the VSMOW/VSLAP scale. Precision and accuracy are maintained at better than ±2‰.

2.4. Noble Gas Analysis

[21] Water samples for noble gas analysis were collected in 3/8″ Cu tubes clamped at both ends and analyzed for He, Ne, Ar, Kr, and Xe isotopes at the University of Michigan using an automated noble gas extraction system connected to a MAP215 mass spectrometer which has been modified to have sufficient mass resolution for measuring $^3He/^4He$ ratios. The mass spectrometer source was operated at an electron trap current of 500 μA. Sampling and measurement procedures are those as reported by *Ma et al.* [2004] with further details on noble gas procedures of *Saar et al.* [2005] and *Castro et al.* [2007].

[22] Noble gases were separated using an Air Equipped cryogenic separator, with gas release points at 35, 65, 170, 200, and 270 K for He, Ne, Ar, Kr, and Xe, respectively. The original technique described by *Saar et al.* [2005] was modified such that the gas sample was inlet into the cryoseparator at a temperature of 280°K and all gases were pumped into the activated charcoal chamber as it was cooled to ~10°K. Gases were then released as the cryoseparator was warmed through the release point of each noble gas. This modification of the earlier one documented by *Saar et al.* [2005] was done to reduce the possibility of interference from one gas upon another in the trapping efficiency of the cryoseparator. With the exception of He, all other noble gas isotope ratios were identical to air within measurement precision. Noble gas volume measurements are estimated to be accurate to 1.5%, 1.3%, 1.3%, 1.5% and 2.2% for He, Ne, Ar, Kr, and Xe, respectively (1σ).

3. Results and Discussion

[23] Results of the full set of sonde and noble gas measurements of over a 1 year period are shown in Figure 3. A detailed blowup of the data for the period corresponding to days 167 to 175 that captures Hurricane Ike is shown in Figure 4. Air temperature and precipitation data from the AAMA weather station are plotted along with sonde measurements of water depth, pH, ORP, DO, water temperature

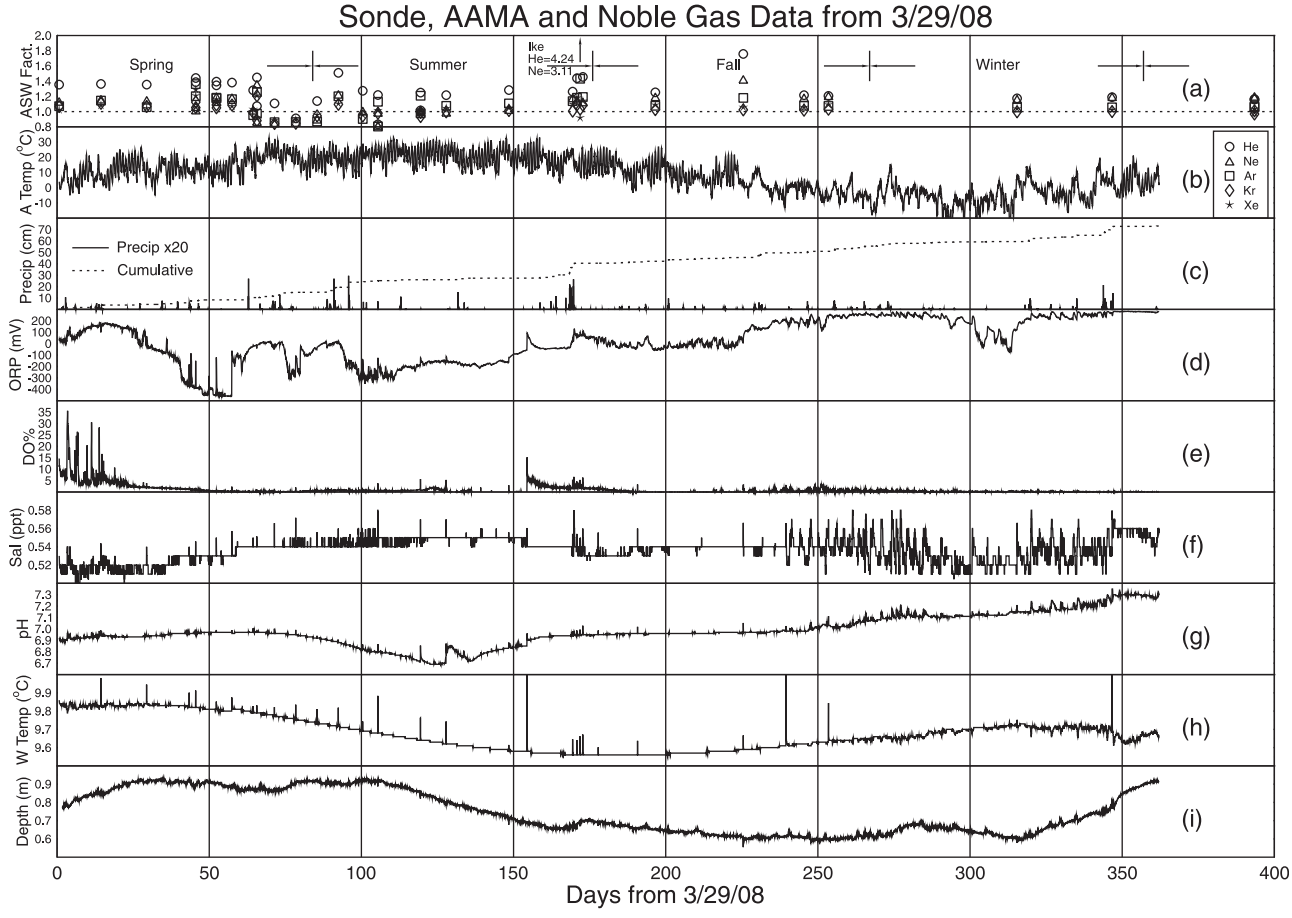

Figure 3. Noble gas, sonde, and meteorological data over the entire course of the experiment: (a) noble gas volumes (He, Ne, Ar, Kr, and Xe) normalized to air-saturated water at 9.7°C at an altitude of 300 m (errors $\pm 1\sigma$), (b) AAMA measured air temperature, (c) AAMA reported precipitation times 20 (solid line) and cumulative (dashed line), in cm, (d) oxidation reduction potential (see text for description of discontinuities due to sonde repositioning), in mV, (e) dissolved oxygen as a percentage of saturation, (f) salinity, in parts per thousand (ppt), (g) measured pH, (h) measured water temperature, in °C, and (i) depth of the sonde sensor array with discontinuities due to repositioning removed (see text), in m.

and salinity. Noble gas concentrations are plotted normalized to air-saturated water at 300 m altitude and 9.7°C, which correspond to the local recharge altitude and average ground temperature, respectively. Tables of meteorological, sonde, stable isotope and noble gas concentration data are given in the auxiliary material.[1]

3.1. Air Temperature Versus Water Table Temperature

[24] Air temperature from the AAMA weather station (Figure 3b) is a maximum in midsummer at around day 120 and is a minimum in midwinter at around day 300. The range in temperature, including diurnal variations, exceeds 40°C. In contrast, the groundwater temperature measured by the sonde (Figure 3h) was highest around day 30 (mid spring) and a minimum around day 200 (fall), with an average value of 9.67°C and a standard deviation of 0.09°C. This indicates that the large annual temperature fluctuations seen in southern Michigan are greatly attenuated at the local water table and water temperature changes lag air temperatures by 8–9 months. There are occasional upward spikes in water temperature of ~0.1–0.2°C, but these are sampling artifacts caused by heat dissipation in the electric pump used to collect water for noble gas analysis. This can be seen in more detail in Figure 4h, which shows that the bulk of the heat is dissipated within a 1–2 h after sampling. Generally, there is little indication of water temperature variation being caused by large precipitation events (e.g., Figure 4h for days 168 and 169), however, there is a very small dip in water temperature (~0.03°C) on day 3 that correlates with an early spring rainstorm. This demonstrates that, to an excellent approximation, infiltrated rainwater has reached ambient temperature by the time it reaches the water table.

3.2. Precipitation

[25] Precipitation at the AAMA weather station is plotted in Figure 3c. Cumulative precipitation in cm is plotted as a dashed line and continuous measurements are plotted as a solid line, with the continuous measurements being multiplied by a factor of 20 for the purposes of clarity. In the AAMA data, snow precipitation has been converted to

[1]Auxiliary materials are available in the HTML. doi:10.1029/2011WR010951.

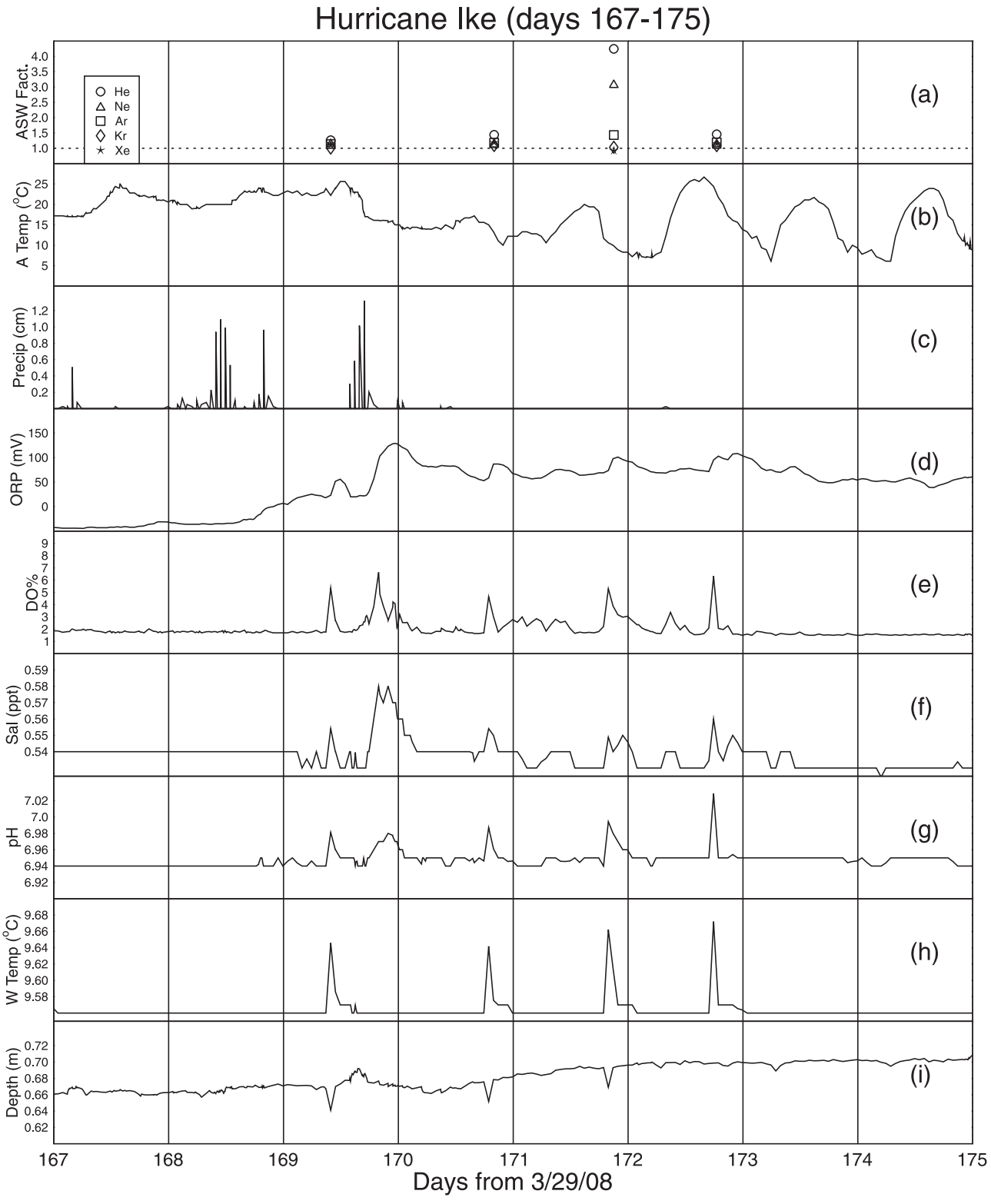

Figure 4. Detailed view of the data shown in Figure 3 during the passage of Hurricane Ike. Plotted values are as in Figure 3, except Figure 4c, where precipitation is not multiplied by 20 and no cumulative precipitation is shown.

the liquid water equivalent. The bulk of the annual precipitation occurred during spring and in one exceptional late summer rainstorm, the remnants of Hurricane Ike. The AAMA site is approximately 12 km south of the monitoring well site, which means that it is possible for some isolated thunderstorms to appear at the AAMA station without affecting the area around the well. However, the most important precipitation events affected the entire southeastern

Michigan region and the AAMA data should be generally representative for the study site.

[26] The single most important precipitation event was Hurricane Ike, a category 4 hurricane that made landfall near Houston Texas and moved north along the Mississippi River valley. Although the storm reduced in strength as it moved north, significant outer rain bands passed over southern Michigan on 13 and 14 September 2008 (days 168 and 169). A detailed view of the AAMA meteorological and sonde data is shown in Figure 4 and a sequence of daily water samples were taken to document the effects of this rainstorm.

3.3. Dissolved Oxygen

[27] Dissolved oxygen (DO) as a percentage of groundwater O_2 saturation is shown in Figure 3e. As noted above, the DO sensor's membrane has a limited effective lifetime and we estimate that the readings are only accurate for 20–30 days after the initial sonde deployment on day 0 and when the membrane was replaced on day 154. In early spring, there are several upward spikes of DO that correlate with significant rainfall. DO levels at the water table in the monitoring well are typically near 45% saturation [cf. *Sun et al.*, 2008] and drop significantly with depth. It can be seen from Figure 3e, that DO values in the vicinity of the sonde sensors (~0.8–0.9 m at that time) can briefly rise to 20–30%, but fall subsequently to <10%, presumably as the free O_2 is consumed by microbial respiration. After the sonde was repositioned and the DO sensor membrane was replaced on day 154, DO levels remained quite low, even during the heavy rainfall of Hurricane Ike. However, there was a small DO response late on day 169, as shown in Figure 4e. The remaining spikes in DO values in Figure 4e are related to mixing within the well during water sampling for noble gas analysis.

3.4. Salinity

[28] Salinity, in parts per thousand (ppt), was estimated from specific conductivity measurements and is shown in Figure 3f, with a detailed view in Figure 4f. Values of salinity vary within a narrow range near 0.55 ppt, with a significant increase in variability in late fall and the winter of 2008–2009. The generally narrow range of salinity values argues against any large-scale drift in calibration for this sensor. One possibility for an increase in salinity variance during the cold season is that the monitoring well is within 10 m of a paved road and it is likely that small quantities of road salt, commonly applied during snow storms, migrates to the water table during rain storms and/or periods of snow melt. Figure 4f shows a distinct increase in salinity due to Hurricane Ike late on day 169. The remaining variations in Figure 4f are brief disturbances correlated with groundwater sampling.

3.5. pH

[29] The pH data show that groundwater at the sonde was nearly neutral for most of the spring, with a slow drift to slightly acidic conditions in midsummer (Figure 3g). Generally, transient sampling artifacts for pH dissipated within a few hours of groundwater sampling (e.g., Figure 4g), but on day 127, there was a steep increase in pH which took about one week to decay back to original values. In late summer and throughout the fall, pH returned to near neutral levels, but during the winter of 2008–2009, pH gradually climbed to more alkaline levels, reaching values near 7.3 by the end of the experiment. If pH is controlled, at least in part, by the concentration of carbonic acid, i.e., the dissolved form of CO_2, then the relatively high pH values during winter suggests a relatively low pCO_2 level near the water table during winter and a higher value during summer. A recent study by *Jin et al.* [2009] documented seasonal variations in pH and pCO_2 in Michigan watersheds. The observed pattern of lower pH in summer with higher pH in winter also corresponded to high pCO_2 in summer, with low values of pCO_2 being measured in winter. Alternatively, the pH sensor may have undergone a slow long-term drift in calibration.

3.6. Oxidation Reduction Potential

[30] By far the most variable parameter measured was ORP, which is the voltage difference between an Ag and a Pt electrode in contact with groundwater. Positive values indicate oxidizing conditions, while negative values occur when the water is more reducing. Values in mV are plotted in Figure 3d. Conditions were relatively oxidizing during early spring, but by day 40, there was a steep drop in ORP, indicating reducing conditions, likely due to an increase in organic content in the groundwater. Experience in the wastewater treatment industry suggests that methane production may take place when ORP values are in the range of –175 to –400 mV [*Gerardi*, 2007] and these ORP conditions prevailed for much of mid spring. On day 57, the sonde-pump assembly was raised to prevent corrosion on connections above the sonde and ORP values jumped back to nearly neutral values. This indicates that there was a significant gradient in oxidizing conditions near the water table at this time. There was a sudden drop in ORP in late spring, a recovery to values near zero, and then a decline to reducing conditions throughout most of the summer. When the sonde was raised on day 154, there was a small increase in ORP, which was significantly less than the drop seen for on day 57. Since the distance that the sonde was moved was the same on days 57 and 154, the vertical ORP gradient was less in late summer than in late spring. Figure 4d shows the rapid response of ORP to the infusion of groundwater following Hurricane Ike, with values increasing from 0 to more than 100 mV in less than 2 days. ORP remained relatively steady in early fall, but began to rise to nearly 300 mV by early winter. Aside from a brief drop shortly after day 300, oxidizing conditions prevailed with ORP values near 300 mV through the rest of the winter of 2008–2009.

3.7. Water Depth

[31] As noted earlier, the raw water depth data were negatively correlated with atmospheric pressure and it was necessary to remove this component from the depth record in order to document true variations in the water table. Discontinuities in the record on days 57 and 154 have also been removed in the plot shown in Figure 3i. The general pattern shows a relatively high water table (sonde depth >0.9 m) through spring and early summer, with a gradual decline in depth to values below 0.6 m by late fall. Depth values greater than 0.9 m were reached again by the beginning of spring in 2009. Figure 4i shows the direct response

of the water table within 2 days of the major rainfall associated with Hurricane Ike and it also shows the brief drawdown caused by the use of the water pump during the sampling episodes shortly after Hurricane Ike.

3.8. Noble Gas Concentrations

[32] Noble gas concentrations are displayed in Figure 3a, with individual noble gas values normalized to expected ASW values for standard air at an altitude of 300 m above sea level for a temperature of 9.7°C, which is the annual average water temperature measured by the sonde. If only an ASW component in equilibrium with standard air at 100% relative humidity were present, all noble gas values would plot very close to a value of 1 (dashed horizontal line in Figure 3a). Any "excess air" component, i.e., noble gases with relative concentrations equivalent to standard air incorporated as dissolved bubbles [*Heaton and Vogel*, 1981], would show up as elevated normalized concentration values for all noble gases, but with He and Ne values significantly higher than for the heavier noble gases.

[33] In the early part of the record, the heavy noble gases cluster around a value of ~1.1, with Ne trending a little higher and He near values of 1.4 (Figure 3a). This is similar to data from a nearby domestic well presented by *Hall et al.* [2005]. Both in that study and in a later study that analyzed noble gases in a vertical traverse in the monitoring well [*Sun et al.*, 2008], the presence of a persistent He excess in this aquifer, over and above that which can be explained by an excess air component, is well documented. However, in late spring (near day 65), there is a distinct drop in the concentrations of all noble gases. He still has a normalized value higher than the heavier noble gases, but most noble gases have concentrations that drop significantly below ASW for a period of about 20 days.

[34] Normalized noble gas concentrations rebounded by late summer to values close to those seen in early spring. The effects of the major precipitation from Hurricane Ike (days 168 and 169) are shown in Figure 3a and in more detail in Figure 4a. Late on day 171, a groundwater sample was collected that displayed extremely large excesses of He and Ne that plot off scale in Figure 3a and are shown in Figure 4a. Notably, the Xe concentration is below that expected for ASW at 9.7°C and the implications of this are discussed in more detail below. Several groundwater samples had elevated Ne concentrations during the fall of 2008 (Figure 3a). However, following Hurricane Ike, the heavy noble gases cluster near a value of one, indicating that a significant shift in conditions near the water table occurred during that major recharge event.

3.9. Stable Isotopes

[35] The results from stable isotope analysis of groundwater samples are shown in Figure 5 in the form of a plot of δD versus $\delta^{18}O$. The samples analyzed plot close to the

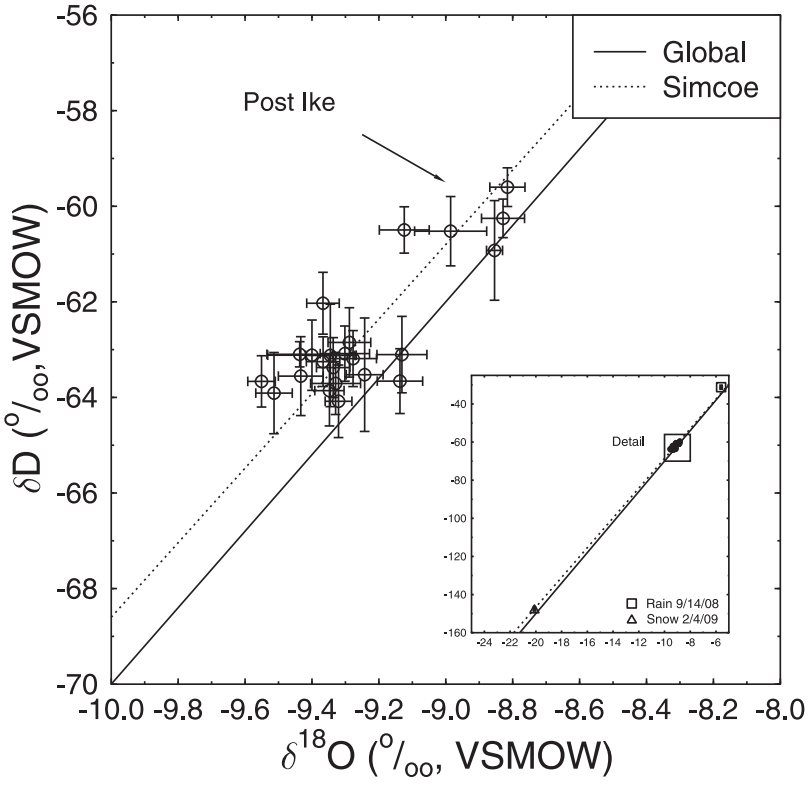

Figure 5. Oxygen and hydrogen isotope ratio values plotted relative to VSMOW (per mil). Errors are $\pm 1\sigma$. The solid line is the global meteoric line [*Craig*, 1961], and the dashed line is the regional line for Lake Simcoe, Ontario [*Dansgaard*, 1964]. All samples taken after Hurricane Ike cluster around heavier isotope values. The inset shows groundwater data (within small rectangle) relative to rain collected on 14 September 2008 (during Hurricane Ike) and snow collected on 4 February 2009.

global meteoric line of *Craig* [1961]. As noted by *Ma et al.* [2004], groundwater from the Glacial Drift aquifer in SE Michigan plot close to the regional meteoric line for Lake Simcoe in S. Ontario [*Dansgaard*, 1964] and all of our data plot very close to that line. Samples taken in the early portion of the experiment cluster very tightly near a δD value of –63‰ and a $\delta^{18}O$ value of –9.3‰. However, subsequent to the heavy rainfall from Hurricane Ike, δD and $\delta^{18}O$ values shifted to heavier values by ∼2‰ and ∼0.4‰, respectively. Also shown in Figure 5 in an inset are the results of stable isotope analyses of precipitation at the study site collected 14 September 2008 (rain during Hurricane Ike) and 4 February 2009 (snow). Both precipitation samples plot very close to the regional meteoric line and it is clear that the groundwater samples can be modeled as a weighted average of contributions from rain and snow, with the isotopically heavier rain samples providing nearly 75% of groundwater recharge.

4. Interpretation in Terms of NGT Models

[36] Standard NGT models can be employed to interpret our noble gas concentration data in the context of the history of chemical and physical parameter variations measured in the monitoring well over the course of the yearlong study. The results of this analysis, presented below, show that each one of the models can adequately explain a portion of the record, but none of them, independently, is able to correctly reproduce conditions near the water table for the entire year.

4.1. Unfractionated Air Model

[37] As noted above, the simplest NGT model is the unfractionated air (UA) model that combines an ASW component [*Mazor*, 1972] with an excess air component [*Heaton and Vogel*, 1981], where the excess air component has a noble gas composition that is identical to standard air. More specifically, the UA model can be described by

$$C_i = ASW_i + AZ_i \quad (1)$$

where C_i denotes the concentration of the ith noble gas in groundwater (i = Ne, Ar, Kr, Xe); ASW_i is the temperature-dependent air-saturated water concentration for the ith noble gas; A is the volume of incorporated excess air per gram of water; and Z_i is the volume fraction of the ith noble gas in dry air. We used inverse techniques developed by *Ballentine and Hall* [1999] to estimate temperature and excess air, with the modification that the excess air parameter A was constrained to be nonnegative. Results of this analysis are shown in Figure 6. Fitted NGT values are plotted in Figure 6a, and the excess air component is plotted in the ΔNe format (defined by *Aeschbach-Hertig et al.* [2002b]), where ΔNe is defined as $Ne_{measured}/Ne_{ASW} - 1$ (Figure 6b). The Ne_{ASW} component used to define ΔNe is that part of the Ne concentration that is used by a particular NGT model that is used to derive temperature.

[38] Throughout most of the spring, UA model NGT values are below ambient groundwater temperature, with values trending down below 5°C by the end of the season. These NGT values are similar to both those found for samples from the nearby domestic well documented by *Hall et al.* [2005], as well as the UA model NGTs for zero-aged groundwater samples from the Marshall Sandstone in southern Michigan [*Ma et al.*, 2004]. The "coldest" apparent NGT samples were sampled well after the major snowmelt, as indicated by air temperatures at the time (see Figure 2b). Given that most measured groundwater parameters respond to major precipitation events within hours or, at most a few days, as discussed in section 3 (see also Figures 2 and 3), it is highly unlikely that the low UA model NGT values are caused by the earlier influx of cold water, as suggested by *Klump et al.* [2006] in their comment on the *Hall et al.* [2005] study [see also *Hall et al.*, 2006]. Indeed, groundwater temperature at this time is near its yearly maximum of about 9.85°C, indicating that water reaches ambient temperature during infiltration in the unsaturated zone, well before it reaches the water table.

[39] In late spring and early summer (around day 70), UA model NGT values change dramatically, with most values well in excess of the ambient groundwater temperature. Error estimates are high because Ne concentrations are so low that the UA model collides with the nonnegativity constraint for excess air. This is indicated by significantly negative ΔNe values, as shown in Figure 6b. By midsummer, however, UA model NGTs return to values near or below groundwater temperature and ΔNe values return to positive values, indicating a rise in Ne concentrations. The behavior of noble gas concentrations in early summer is difficult to explain using the standard UA model, but it is likely that a significant degassing event [*Brennwald et al.*, 2003, 2005; *Aeschbach-Hertig*, 2008; *Cey et al.*, 2008, 2009] occurred, which can explain both the anomalously high UA model NGTs as well the negative ΔNe values. This is discussed in more detail below.

[40] By late summer, UA model NGT values returned to levels similar to those seen in early spring, but the major recharge event during Hurricane Ike caused a significant shift in the noble gas concentrations in the monitoring well. Interestingly, on day 171, just 2–3 days after the most significant rain storms associated with the hurricane (Figure 4c), the groundwater sample with very high He and Ne values along with relatively low Xe (Figure 4a) yielded a UA model NGT that was extremely close to the prevailing daytime surface air temperature. The simplest explanation for this anomalous sample is that it represents a quantity of groundwater that reached the water table so quickly that it not only entrained a significant volume of bubbles containing excess air, it also had insufficient time to equilibrate with the ambient temperature at the water table. Although extremely high UA model NGT values did not persist past the rainfall from Hurricane Ike, NGT values do not drop significantly below groundwater temperature and thus did not display the bias to low temperatures observed in previous years [see, e.g., *Ma et al.*, 2004; *Hall et al.*, 2005]. This indicates that Hurricane Ike caused an important shift in conditions near the water table for the remainder of the yearlong study as was also clearly shown by our stable isotope results, which display a dramatic shift in their signature following this major storm event (see Figure 4).

4.2. Oxygen Depletion Model

[41] Another perspective on the noble gas concentration results can be obtained using the oxygen depletion (OD)

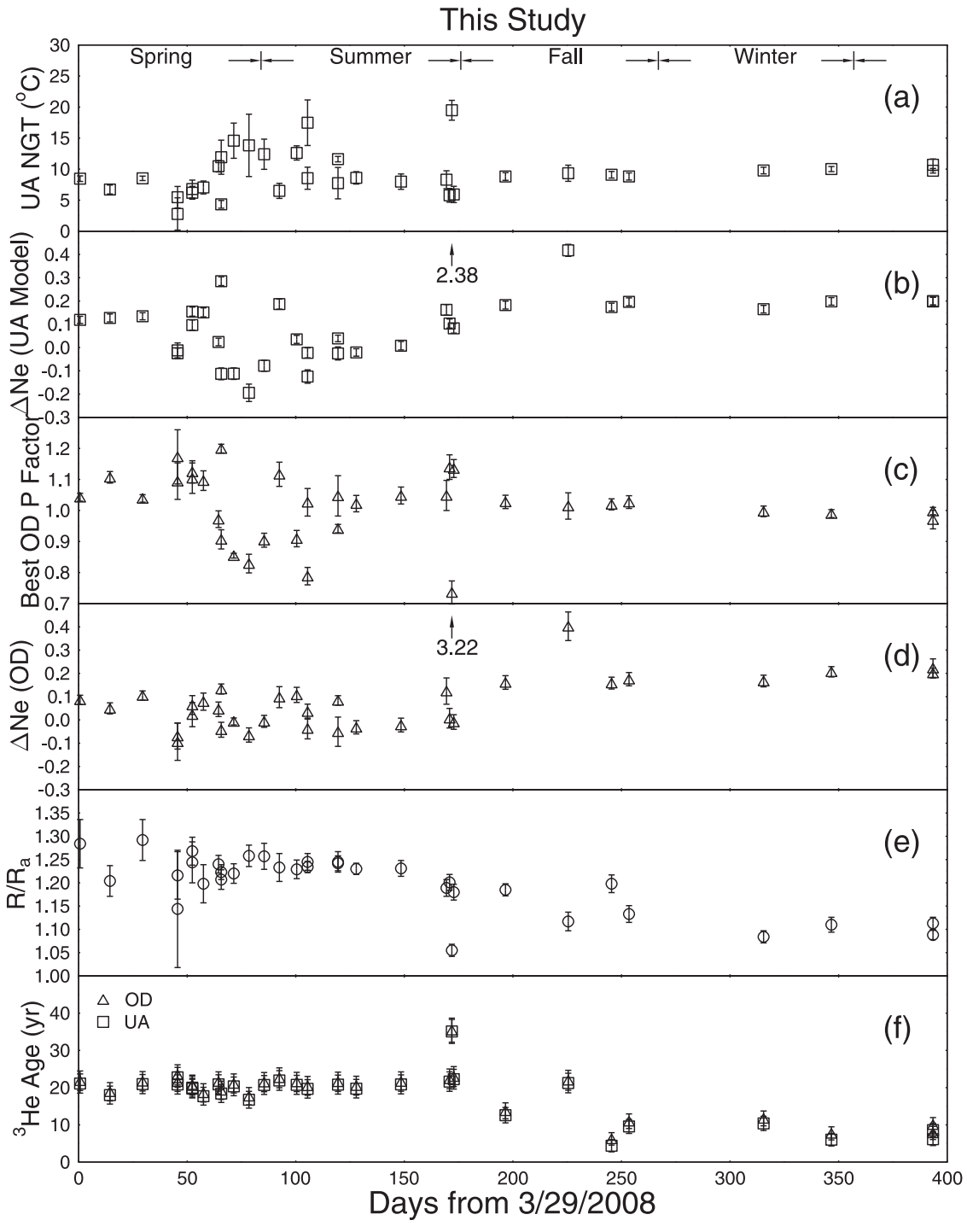

Figure 6. Noble gas results interpreted in terms of the unfractionated air (UA) and oxygen depletion (OD) models plotted as a function of days from 29 March 2008: (a) fitted noble gas temperatures (NGTs), in °C, (b) UA model ΔNe values, (c) OD model fitted pressure factors assuming a true equilibration temperature of 9.7°C, (d) OD model ΔNe values, (e) $^3He/^4He$ values (R), normalized to the atmospheric value, and (f) apparent ^3He ages using both OD and UA model ASW values (see text for details). All errors are $\pm 1\sigma$.

model first proposed by *Hall et al.* [2005] and further utilized by *Castro et al.* [2007] and *Sun et al.* [2008, 2010]. The OD model relaxes the assumption that soil air has a standard atmospheric composition due to the consumption of oxygen in the unsaturated zone. The OD model of *Hall et al.* [2005] can be written as

$$C_i = ASW_i P_{OD} + AZ_i \quad (2)$$

where P_{OD} is a pressure adjustment factor that accounts for the loss of O_2 in the unsaturated zone that can result from plant respiration, microbial action [see, e.g., *Cey et al.*, 2009] and/or other chemical reactions. In the case of the OD model, the ASW component of Ne as modified by the P_{OD} factor is used to calculate of ΔNe. A loss of active gases, which was documented for the monitoring well by *Sun et al.* [2008], leads to an increase in the partial pressures of all remaining gases, including, specifically, noble gases. With a net O_2 loss, $P_{OD} > 1$; when $P_{OD} = 1$, the OD model reduces to the UA model. As noted by *Sun et al.* [2010], varying P_{OD} from a value of 1 is mathematically equivalent to changing the assumed recharge altitude. *Ballentine and Hall* [1999] showed that the inverse problem of simultaneously fitting NGT, excess air and altitude (or, equivalently, P_{OD}) is an ill-posed problem. Therefore, it is not feasible to simultaneously fit temperature, excess air and P_{OD} for an individual sample. Instead, *Hall et al.* [2005], *Castro et al.* [2007], and *Sun et al.* [2008, 2010] fitted a single optimal P_{OD} value to a suite of samples from a single aquifer, assuming that the value is relatively constant over time.

[42] Here, the actual groundwater temperature is known and rather than fitting the entire suite of temperature, P_{OD} and excess air (A), it is possible to assume a fixed water temperature value and instead fit just P_{OD} and A. This is a well-posed problem and we show the optimal individual P_{OD} values subject to the constraint that $A \geq 0$ (Figure 5c). For the purposes of this analysis, we have fixed the NGT value to 9.7°C, which is the average annual groundwater temperature, while looking for the P_{OD} value that is compatible with the true groundwater temperature. Thus, an optimal P_{OD} value of 1 indicates that soil air has an O_2 partial pressure that is equivalent to that of standard air and consequently, that the UA model would yield an accurate NGT value. A P_{OD} value greater than 1 would suggest a significant loss of O_2 in the unsaturated zone.

[43] In early to midspring, fitted P_{OD} values are all above 1, with many values near 1.1, close to the value estimated by *Hall et al.* [2005] for the nearby domestic well. However, there is a dramatic fall in P_{OD} by the end of spring and earliest summer, with some values dropping to about 0.8. Simultaneously, ΔNe values derived from the fitted excess air parameter (A) drop to negative values, pointing to a significant Ne deficiency in these samples (Figure 6d). By midsummer, P_{OD} values rise again to values above 1, but ΔNe remains relatively low.

[44] Hurricane Ike in late summer has a dramatic effect on both P_{OD} and ΔNe values. The sample collected on day 171 has both an exceptionally low P_{OD} value of 0.736 and a ΔNe value of 3.22 (Figures 5c and 5d), but the optimal P_{OD} values soon stabilize to values near 1 and remain unchanged for the rest of the year. Although the extremely high concentrations of Ne seen during Hurricane Ike are not sustained, there is a distinct shift to higher ΔNe values (Figure 5d) for the entire fall and winter seasons (Figure 5d). There is independent confirmation of the effects of excess air from He isotope data. The $^3He/^4He$ ratio R is plotted in Figure 6e, normalized to the atmospheric ratio R_a. For the first half of the record, R/R_a values are typically about 1.2, even during the period of low P_{OD} values in late spring and early summer. However, the unusual Hurricane Ike sample with an extremely elevated ΔNe value (day 171) has an R/R_a value very close to 1 and for the remainder of the year, this ratio shifts to values closer to 1.1, distinctly lower than those of spring and summer. This indicates that the apparent infusion of excess air also introduced a significant quantity of He with atmospheric isotopic composition and this elevated level of excess air persisted for the remainder of the year. In addition, approximate $^3He/^3H$ ages are also shown in Figure 6f. Generally, ages derived from tritiogenic ^3He are generally constant at about 20 years in the early part of the record but ages drop significantly after the recharge event during the passage of Hurricane Ike. Two sets of ages were calculated, with one assuming an ASW component based on the UA model and the other based on the OD model. The assumptions used to derive these apparent ages are discussed in section 5.

4.3. CE Model

[45] Neither the UA nor OD models can directly address the possibility of water degassing via bubble formation in the saturated zone. In contrast, the closed system equilibration (CE) model of *Aeschbach-Hertig et al.* [2000] can be interpreted to allow for the possibility of degassing [*Aeschbach-Hertig et al.*, 2008]. The original CE model allowed for partial dissolution of noble gases from entrapped air bubbles, with the remainder of the bubble becoming separated from the groundwater. In practice, the four noble gas concentrations (Ne, Ar, Ke, and Xe) are fitted by adjusting three parameters, temperature, an initial EA concentration designated "A", and a fractionation factor "F" that combines the factors of compression of the entrapped bubble and the fraction of the bubble that escapes. The CE model can be described by

$$C_i = ASW_i\left(\frac{ASW_i + AZ_i}{ASW_i + FAZ_i}\right) \tag{3}$$

where the C_i, Z_i, and ASW_i parameters are the same as previously indicated for the UA model equation. The A parameter represents the total initial volume of trapped excess air. The fractionation factor F is equal to the ratio of the final bubble value (designated B by *Aeschbach-Hertig et al.* [2008]) to the original volume A. In the CE model with no degassing, A is nonnegative and $A \geq B$, thus $0 \leq F \leq 1$. However, if an air bubble grows, $A \leq B$ and $F \geq 1$. This can successfully model the case where there is some initial excess air along with bubble growth and escape, leading to net noble gas loss. In the limit where $A = 0$, then $F \rightarrow \infty$, which reduces the CE model to the degassing model of *Brennwald et al.* [2003]. When $F = 0$, the CE model becomes the UA model and when $F = 1$ and $A \rightarrow \infty$, the CE model approaches the OD model with no excess air [*Sun et al.*, 2010].

[46] The CE model analysis results are shown in Figure 7, which includes fitted NGTs (Figure 7a), F values (Figure 7b), and ΔNe values (Figure 7c). Many of the NGT values have extremely large error estimates and this is due to an inherent problem with nonuniqueness that sometimes affects the CE model, as previously discussed by Sun et al. (2010). In other words, the CE model allows for a large range of F, A and NGT values that can model nearly identical noble gas data. This problem is especially

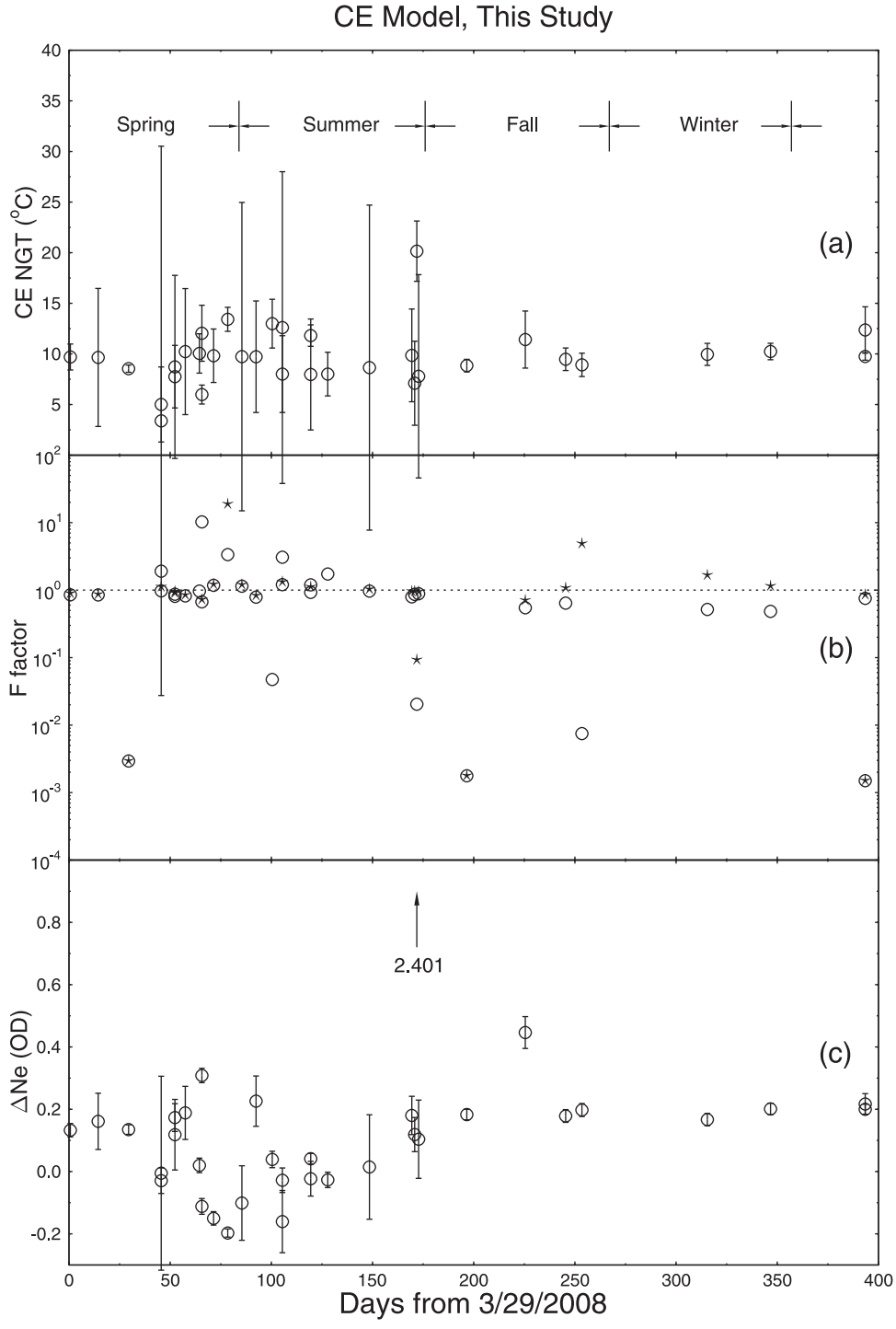

Figure 7. Noble gas results interpreted using the closed-system equilibration (CE) model of *Aeschbach-Hertig et al.* [2008] : (a) fitted NGTs, in °C, (b) fitted F factor, with values >1 indicating outgassing (stars are values $+1\sigma$ error estimate), and (c) CE model ΔNe values. All errors are $\pm 1\sigma$.

evident in the samples from spring and summer (Figure 7a). It should be noted that most, but not all, of the CE model NGT values are not significantly different from the true average groundwater temperature of 9.7°C. However, for numerous analyses, the error estimates are so large as to render the NGT values ineffective as a temperature proxy. The Hurricane Ike sample collected on day 171 yields a relatively high NGT value, comparable to the value obtained using the UA model.

[47] Fitted F values are plotted as circles in a logarithmic plot (Figure 7b), with the star symbol representing the F value plus a 1σ error estimate. Several of the early spring samples have F values near 1 (possibly compatible with the OD model), but many of the late spring and early summer

samples have F values above 1, indicating that at that time, the CE model fits require degassing in these samples. In contrast, the fall and winter samples have F values below 1, with some very close to 0, indicating that the CE model for these samples is trending toward the UA model.

4.4. NGT Models: Discussion and Summary

[48] None of the NGT models examined here can independently explain the entire set of noble gas data acquired from the monitoring well over the entire course of the yearlong study. For the early to midspring samples, results seem to be best explained by the OD model with P_{OD} values ranging from 1.04 to 1.20 (Figure 6c). By late spring and early summer, ORP values dropped precipitously, indicating a marked switch to reducing conditions, and by day 70, several samples exhibited strong signs of having lost noble gases via the mechanism of bubble formation. For these samples, the CE model is most appropriate, but its extremely large NGT error estimates preclude the use of this data as an effective temperature proxy. However, even during this period with low ORP values, some noble gas samples resemble those taken in early spring, suggesting that the degassing seen in late spring and early summer may have only affected a shallow portion of the aquifer near the water table.

[49] By late summer, ORP values were slowly climbing back toward oxidizing conditions and noble gas concentrations returned to values similar to those seen in early spring. The large-scale recharge event during the passage of Hurricane Ike injected a significant quantity of excess air and also shifted the stable isotope ratios to distinctly heavier values. One sample taken during Hurricane Ike is compatible with the UA model assuming that the water traversed the unsaturated zone so quickly that it did not reequilibrate with conditions prevailing at the water table, an effect similar to what was found in artificial recharge ponds [*Clark et al.*, 2005; *Clark*, 2007] when recharge rates were particularly high. The effects of Hurricane Ike linger for the rest of the study, with fitted P_{OD} values near 1, and thus, over that period, the UA model gives reasonable NGT values. After Hurricane Ike, ΔNe values are significantly higher than those seen earlier in the record and the presence of extra excess air is confirmed by a distinct drop in R/R_a values.

[50] *Sun et al.* [2010] argued that although absolute temperatures estimated from noble gas concentrations are sensitive to the specific NGT model that is used, temperature changes are remarkably consistent between models and that it is likely that NGT paleoclimate reconstructions can be robust measures of changes in average ground temperature and by extension, mean annual air temperature (MAAT). However, as shown in this yearlong noble gas record, this is clearly not the case over the timescale of weeks or months. For example, in this study, UA model NGT values range from 2.8°C to an extreme value of 19.4°C immediately following Hurricane Ike (see Figure 6a) despite the fact that the groundwater temperature averaged 9.7°C, with variations of less than a few 10ths of a degree. Implicit in the *Sun et al.* [2010] analysis, however, is that the basic conditions controlling noble gas concentrations within groundwater remain reasonably constant. This may be approximately true when averaged over a period of years, but when examined in detail over a period of days, weeks and months, there are significant changes in conditions that can cause substantial swings in NGTs that do not reflect true temperature changes.

[51] There is evidence that, on average, conditions in the Glacial Drift aquifer in Southern Michigan are compatible with the OD model with a value of P_{OD} of $\sim$1.1, as suggested by *Hall et al.* [2005]. This view is bolstered by an analysis of noble gas data collected in connection with the study of *Sun et al.* [2008]. In that study, 16 groundwater samples were taken from the monitoring well in a vertical traverse on 11 February 2007. An analysis of that noble gas concentration data is shown in Figure 8, in the same format as was used in Figure 6, but values of UA model NGTs, UA model ΔNe, fitted P_{OD}, and OD model ΔNe are now plotted versus sampling depth in Figures 8a, 8b, 8c, and 8d, respectively. There, it can be seen that in February of 2007, the fitted P_{OD} values are remarkably consistent, with an average value of 1.135 and a standard deviation of 0.028, in excellent agreement with the estimate by *Hall et al.* [2005]. In addition, OD model ΔNe values are very low, suggesting that, using this NGT model, there was nearly a total absence of significant excess air at that time. Values for R/R_a and tritiogenic ^{3}He ages are shown in Figures 8e and 8f, respectively.

[52] Finally, the striking negative correlation between measured water depth and atmospheric pressure (Figure 1) suggests that rapid gas transport within the unsaturated zone is not observed, corroborating a hypothesis made by *Sun et al.* [2008] to account for a lack of vertical concentration gradient in the monitoring well for excess ^{4}He. There is ample evidence throughout our yearlong record (Figures 2 and 3) that groundwater chemistry responds rapidly to precipitation events, with effects often seen within hours. Yet, the slower response of the gas phase in the unsaturated zone suggests that there is a significant buffer between the saturated zone and the atmosphere.

5. Apparent ^{3}H/^{3}He Groundwater Ages

[53] Elevated R/R_a values, up to 1.29 measured in this study and 1.56 for that of *Sun et al.* [2008] can be interpreted as being due to tritium decay. Although no tritium measurements were made on the water samples for either this study or *Sun et al.* [2008], an approximate estimate of current tritium levels can be derived from a 1986 measurement from groundwater from the nearby recharge area of the Marshall Sandstone [*Dannemiller and Baltusis*, 1990]. Using their measured value of 22 tritium units (TU), the expected current tritium levels for 2007 and 2008 would be 6.8 and 6.5 TU, respectively. A terrigenous R/R_a value of 0.05 was used, which is at the high end of the crustal range assumed by *Ma et al.* [2005], but an error estimate of $\pm$0.05 was also assumed therefore encompassing any likely range of crustal and possible mantle components for this area [*Castro et al.*, 2009]. Using the above tritium values and assuming a terrigenous R/R_a value of 0.05, groundwater ages were calculated following *Schlosser et al.* [1989]. For the purposes of calculating error estimates on these ages, a 20% error was assumed for the present tritium value.

[54] Two separate models for estimating the ASW component were used, the UA model and the OD model

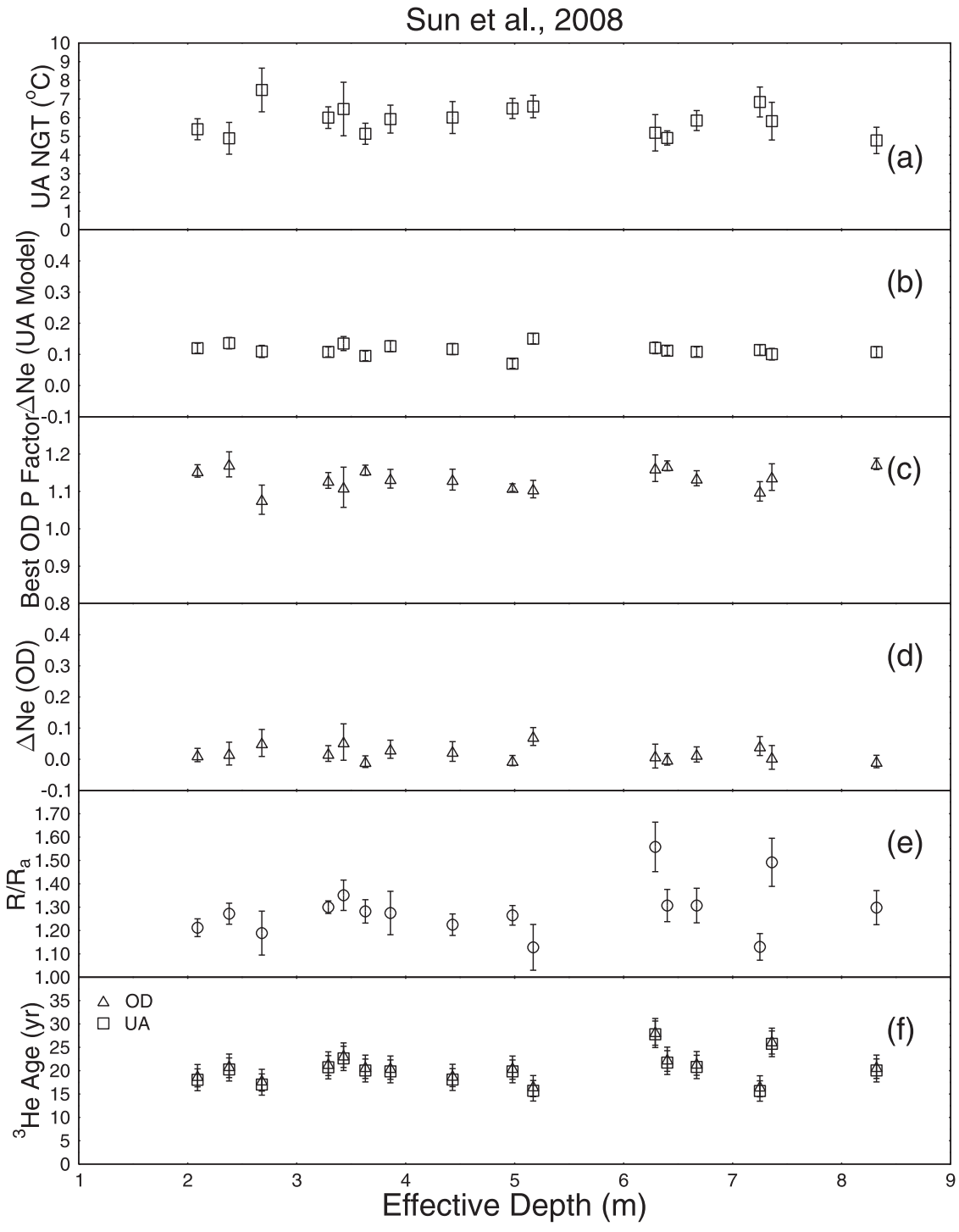

Figure 8. Noble gas results for the monitoring well from *Sun et al.* [2008] interpreted in terms of the UA and OD NGT models, plotted as a function of effective sampling depth (m): (a) fitted UA model NGTs, in °C, (b) UA model ΔNe values, (c) fitted OD model pressure factors, assuming a true groundwater temperature of 9.7°C, (d) OD model ΔNe values, (e) $^3He/^4He$ values (R), normalized to the atmospheric value, and (f) apparent ^3He ages using both OD and UA model ASW values (see text for details). All errors are $\pm 1\sigma$.

assuming an average P_{OD} value of 1.14. In both cases, the temperature used to calculate the ASW component was the groundwater average of 9.7°C. The resulting calculated ages are given in Table S5 of the auxiliary material and are shown in Figures 6f and 8f. All ages are relative to 2008. For the samples collected on a single day in 2007 [*Sun et al.*, 2008], there are very consistent apparent ages, with an average age of 21.0 years for the OD model and 20.2

years for the UA model and a range of ages for each model of less than 1 year. In contrast, there is more variability in apparent ages for samples collected in 2008. In the early part of the record, prior to Hurricane Ike, apparent groundwater ages are similar to those found for the 2007 samples, with an OD model age average of 21.7 and for the UA model an average of 20.9, but the range of calculated ages for these samples increased to nearly 6 years. This variability appears not to be correlated with reducing conditions around day 75.

[55] After Hurricane Ike, there is a distinct drop in apparent ages, with the average age after day 245 being 9.1 years for the OD model and 7.5 years for the UA model. A simplistic view of the apparent age change would suggest that the significant recharge event during Hurricane Ike replaced over half of the groundwater in the vicinity of the well. However, the $\sim$0.4‰ shift of $\delta^{18}O$ values toward the rain end-member, as noted above, is much too small a change if Hurricane Ike had had such a dramatic effect on the overall composition of groundwater in the aquifer. Instead, it appears likely that Hurricane Ike significantly affected the composition of gas in the unsaturated zone, which led to a decrease of ^3He concentration near the water table.

[56] Given that the water velocity near the well is estimated at $\sim$3.3 m d^{-1}, groundwater near the water table that originates at the center of the plateau south of the well ($\sim$1.3 km away), should reach the monitoring well within about 1 year. It is difficult to reconcile the high apparent groundwater ages typically seen at the well unless the thickness of the upper aquifer is significantly greater to the south of our study site. This would allow for upward transport of He isotopes via diffusion and/or advection which could account for the relatively high apparent ^3He ages estimated in this study. It is clear though that the injection of significant excess air into the groundwater during Hurricane Ike reduced apparent ages by over 50%. The fact that the apparent ages do not drop to zero is very likely due to a certain level of vertical mixing of water that occurs within the well during sampling as noted in section 2.1. In order for the $^3H/^3He$ ages to drop to zero would require our sampling water to originate solely from within a few centimeters of the water table and this was not the case.

6. Conclusions

[57] The yearlong noble gas study here presented, together with a wealth of continuous physical and chemical measurements is novel and demonstrates that there can be significant changes in physical and chemical conditions near the water table over the space of a year that can have large effects on noble gas concentrations and hence, NGTs. The yearlong record of conditions in the monitoring well shows broad seasonal variations in pH, salinity, water temperature and water table depth. Early in the record, when the DO sensor was operating normally, there is compelling evidence for the consumption of dissolved O_2 within the saturated zone and this drives the DO vertical gradient documented by *Sun et al.* [2008]. This evidence takes the form of a rapid rise in DO immediately after major rainfall, with a subsequent decline in the following days. The noble gas record for early spring and mid to late summer is broadly consistent with the OD model findings of Hall et al., 2005, with typical P_{OD} values of $\sim$1.1, relatively low ΔNe values and high R/R_a values.

[58] The oxidation state of groundwater near the water table, as revealed by the ORP record, shows oxidizing conditions in the early spring, followed by a sharp decline to reducing conditions by late spring and early summer. By mid to late summer, ORP values rose gradually and by late fall and winter, they reached values measured in early spring. The late spring drop of ORP values to reducing conditions coincides with a period of relatively low noble gas concentrations, which appears to have been caused by a degassing event. During this period, the modified CE model of *Aeschbach-Hertig et al.* [2008], with F values above 1, seems to be the best model for NGTs, in that it produces model temperature values consistent with the true groundwater temperature values. However, NGT error estimates are typically too high for the CE model estimates, occasionally complicating its use as a temperature proxy. It should be noted that at the time of the degassing event, the water table was near its highest point in the year, with the water table dropping throughout the summer of 2008. This fact, in addition to the observed return to conditions compatible with the OD model, suggests that the groundwater that was affected by degassing had little long-term impact on the overall inventory of noble gases in the aquifer.

[59] The late summer rainfall from the outer bands of Hurricane Ike introduced a major shift in groundwater conditions. In addition to a rapid rise in the water table, the stable isotope ratios of O and H underwent a significant shift toward heavier values. One groundwater sample taken immediately following the storm had an extremely high ΔNe value and a UA model NGT that was consistent with surface, rather than water table conditions, suggesting that in this instance, recharge was so rapid that the water had insufficient time to reequilibrate with soil prior to being sampled [see also *Clark et al.*, 2005; *Clark*, 2007]. Following Hurricane Ike, ΔNe values remained elevated and UA model NGT values were consistent with actual groundwater temperatures, suggesting that a significant shift in soil air composition took place during the storm, with O_2 concentrations likely being elevated for the fall and winter seasons.

[60] No single NGT model adequately accounts for all details of the variation in groundwater noble gas concentrations seen throughout the yearlong experiment. Taken at face value, a UA model "paleoclimate record" for the year would indicate a very large temperature change, far in excess of the actual temperature variation. It is clear that an NGT model must integrate long-term conditions, averaging many years, before it can give a reasonable estimate of climate conditions. It should also be noted that a combination of changes in soil gas and degassing events greatly complicates many of the basic assumptions needed to calculate an NGT value and it should not be expected that perfect fidelity to any single model should occur in any given aquifer at all times.

[61] **Acknowledgments.** We thank Werner Aeschbach-Hertig as well as two anonymous reviewers for their constructive comments, which led to a much improved manuscript. We thank Lora Wingate for performing the stable isotope analyses. Financial support by the National Science Foundation CAREER award EAR-0545071 is greatly appreciated. We also wish to thank the many undergraduate students who worked on this project as part of the GEOSCI 210 course sponsored by the NSF CAREER award.

References

Aeschbach-Hertig, W., F. Peeters, U. Beyerle, and R. Kipfer (1999), Interpretation of dissolved atmospheric noble gases in natural waters, *Water Resour. Res.*, *35*, 2779–2792.

Aeschbach-Hertig, W., F. Peeters, U. Beyerle, and R. Kipfer (2000), Paleotemperature reconstruction from noble gases in ground water taking into account equilibration with entrapped air, *Nature*, *405*, 1040–1044.

Aeschbach-Hertig, W., M. Stute, J. F. Clark, R. F. Reuter, and P. Schlosser (2002a), A paleotemperature record derived from dissolved noble gases in groundwater of the Aquia Aquifer (Maryland, USA), *Geochim. Cosmochim. Acta*, *66*(5), 797–817.

Aeschbach-Hertig, W., U. Beyerle, J. Holocher, F. Peeters, and R. Kipfer (2002b), Excess air in groundwater as a potential indicator of past environmental changes, in *Study of Environmental Change using Isotope Techniques*, pp. 174–183, Int. At. Energy Agency, Vienna.

Aeschbach-Hertig, W., H. El-Gamal, M. Wieser, and L. Palcsu (2008), Modeling excess air and degassing in groundwater by equilibrium partitioning with a gas phase, *Water Resour. Res.*, *44*, W08449, doi:10.1029/2007WR006454.

Ballentine, C. J., and C. M. Hall (1999), Determining paleotemperature and other variables by using an error-weighted nonlinear inversion of noble gas concentrations in water, *Geochim. Cosmochim. Acta*, *63*(16), 2315–2336.

Beyerle, U., J. Rueedi, M. Leuenberger, W. Aeschbach-Hertig, F. Peeters, R. Kipfer, and A. Dodo (2003), Evidence for periods of wetter and cooler climate in the Sahel between 6 and 40 kyr BP derived from groundwater, *Geophys. Res. Lett.*, *30*(4), 1173, doi:10.1029/2002GL016310.

Brennwald, M. S., M. Hofer, F. Peeters, W. Aeschbach-Hertig, K. Strassmann, R. Kipfer, and D. M. Imboden (2003), Analysis of dissolved noble gases in the porewater of lacustrine sediments, *Limnol. Oceanogr. Methods*, *1*, 51–62.

Brennwald, M. S., R. Kipfer, and D. M. Imboden (2005), Release of gas bubbles from lake sediment traced by noble gas isotopes in the sediment pore water, *Earth Planet. Sci. Lett.*, *235*, 31–44.

Castro, M. C., and P. Goblet (2003), Noble gas thermometry and hydrologic ages: Evidence for late Holocene warming in southwest Texas, *Geophys. Res. Lett.*, *30*(24), 2251, doi:10.1029/2003GL018875.

Castro, M. C., C. M. Hall, D. Patriarche, P. Goblet, and B. R. Ellis (2007), A new noble gas paleoclimate record in Texas—Basic assumptions revisited, *Earth. Planet. Sci. Lett.*, *257*(1–2), 170–187, doi:10.1016/j.epsl.2007.02.030.

Castro, M. C., L. Ma, and C. M. Hall (2009), A primordial, solar He-Ne signature in crustal fluids of a stable continental region, *Earth Planet. Sci. Lett.*, *279*(3–4),174–184.

Cey, B. D., G. B. Hudson, J. Moran, and B. R. Scanlon (2008), Impact of artificial recharge on dissolved noble gases in groundwater in California, *Environ. Sci. Technol.*, *42*, 1017–1023.

Cey, B. D., G. B. Hudson, J. E. Moran, and B. R. Scanlon (2009), Evaluation of noble gas recharge temperatures in a shallow unconfined aquifer, *Groundwater*, *47*, 646–659.

Clark, J. (2007), Behavior of gases during recharge below spreading ponds, in *Proceedings of the 4th Mini Conference on Noble Gases in the Hydrosphere and in Natural Gas Reservoirs*, pp. 43–44, GeoForschungsZentrum Potsdam, Potsdam, Germany, doi:10.2312.GFZ.mga.005.

Clark, J., G. B. Hudson, and D. Avisar (2005), Gas transport below artificial recharge ponds: Insights from dissolved noble gases and a dual gas (SF6 and 3He) tracer experiment, *Environ. Sci. Technol.*, *39*, 3939–3945.

Craig, H. (1961), Isotopic variations in meteoric waters, *Science*, *133*(3465), 1702–1703.

Cypher, J. A., and L. D. Lemke (2009), Multiple working hypotheses in a heterogeneous glacial aquifer system, *Groundwater Monit. Rem.*, *29*(3), 105–119.

Dannemiller, G. T., and M. A. Baltusis Jr. (1990), Physical and chemical data for ground water in the Michigan Basin, 1986–1989, *U.S. Geol. Surv. Open File Rep.*, *90-368*, 155 pp., US Geol. Surv., Denver, Colo.

Dansgaard, W. (1964), Stable isotopes in precipitation, *Tellus*, *16*, 436–468.

Freeze, A. R., and J. A. Cherry (1979), *Groundwater*, 604 pp., Prentice Hall, Englewood Cliff, N. J.

Gehre, M., H. Geilmann, J. Richter, R. A. Werner, and W. A. Brand (2004), Continuous flow $^{2}H/^{1}H$ and $^{18}O/^{16}O$ analysis of water samples with dual inlet precision, *Rapid Commun. Mass Spectrom.*, *18*, 2650–2660, doi:10.1002/rcm.1672.

Gerardi, M. (2007), Oxidation-reduction potential and wastewater treatment, Interstate Water Report, [Available at http://www.neiwpcc.org/iwr/reductionpotential.asp], New England Interstate Water Pollut. Control Comm., Lowell, Mass.

Hall, C. M., M. C. Castro, K. C. Lohmann, and L. Ma (2005), Noble gases and stable isotopes in a shallow aquifer in southern Michigan: Implications for noble gas paleotemperature reconstructions for cool climates, *Geophys. Res. Lett.*, *32*, L18404, doi:10.1029/2005GL023582.

Hall, C. M., M. C. Castro, K. C. Lohmann, and L. Ma (2006), Reply to comment by Klump et al. on "Noble gases and stable isotopes in a shallow aquifer in southern Michigan: Implications for noble gas paleotemperature reconstructions for cool climates," *Geophys. Res. Lett.*, *33*, L24404, doi:10.1029/2006GL028102.

Heaton, T. H. E., and J. C. Vogel (1981), "Excess air" in groundwater, *J. Hydrol.*, *50*(1–4), 201–216.

Hoaglund, J. R., G. C. Huffman, and N. G. Grannemann (2002), Simulation of ground-water flow in the glaciofluvial Saginaw, Parma-Bayport, and Marshall Aquifers, central Lower Peninsula of Michigan, *U.S. Geol. Surv. Open File Rep.*, *00-504*, 36 pp., US Geol. Surv., Denver, Colo.

Holocher, J., F. Peeters, W. Aeschbach-Hertig, M. Hofer, M. Brennwald, W. Kinzelbach, and R. Kipfer (2002), Experimental investigations on the formation of excess air in quasi-saturated porous media, *Geochim. Cosmochim. Acta*, *66*, 4103–4117.

Holtschlag, D. J. (1996), A generalized estimate of ground-water recharge rates in the Lower Peninsula of Michigan, *U.S. Geol. Surv. Open File Rep.*, *96-593*, 37 pp., US Geol. Surv., Denver, Colo.

Holtschlag, D. J. (1997), A generalized estimate of ground-water recharge rates in the Lower Peninsula of Michigan, *U.S. Geol. Surv. Water Supply Pap.*, *2437*, 37 pp.

Jin, L., N. Ogrinc, S. K. Hamilton, K. Szramek, T. Kanduc, and L. M. Walter (2009), Inorganic carbon isotope systematics in soil profiles undergoing silicate and carbonate weathering (southern Michigan, USA), *Chem. Geol.*, *264*, 139–153.

Kipfer, R., W. Aeschbach-Hertig, U. Beyerle, G. Goudsmit, M. Hofer, F. Peeters, J. Klerkx, J.-P. Plisnier, E. A. Kliembe, and R. Ndhlovu (2000), New evidence for deep water exchange in Lake Tanganyika, *Eos Trans. AGU*, *80*(49), Ocean Sci. Meet. Suppl., Abstract OS239.

Klump, S., M. S. Brennwald, and R. Kipfer (2006), Comment on "Noble gases and stable isotopes in a shallow aquifer in southern Michigan: Implications for noble gas paleotemperature reconstructions for cool climates" by Chris M. Hall et al., *Geophys. Res. Lett.*, *33*, L24403, doi:10.1029/2006GL027496.

Klump, S., Y. Tomonaga, P. Kienzler, W. Kinzelbach, T. Baumann, D. M. Imboden, and R. Kipfer (2007), Field experiments yield new insights into gas exchange and excess air formation in natural porous media, *Geochim. Cosmochim. Acta*, *71*, 1385–1397.

Ma, L., M. C. Castro, and C. M. Hall (2004), A late Pleistocene-Holocene noble gas paleotemperature record in southern Michigan, *Geophys. Res. Lett.*, *31*, L23204, doi:10.1029/2004GL021766.

Ma, L., M. C. Castro, C. M. Hall, and L. Walter (2005), Cross-formational flow and salinity sources inferred from a combined study of helium concentrations, isotopic ratios, and major elements in the Marshall aquifer, southern Michigan, *Geochem. Geophys. Geosyst.*, *6*, Q10004, doi:10.1029/2005GC001010.

Mazor, E. (1972), Paleotemperatures and other hydrological parameters deduced from noble gases dissolved in groundwaters: Jordan Rift Valley, Israel, *Geochim. Cosmochim. Acta*, *36*(12), 1321–1336.

Mercury, L., D. L. Pinti, and H. Zeyen (2004), The effect of the negative pressure of capillary water on atmospheric noble gas solubility in ground water and paleotemperature reconstruction, *Earth. Planet. Sci. Lett.*, *223*(1–2), 147–161, doi:10.1016/j.epsl.2004.04.019.

Ozima, M., and F. Podosek (2006), *Noble Gas Geochemistry*, 2nd ed., 304 pp., Cambridge Univ. Press, Cambridge, U. K.

Rasmussen, T. C., and L. A. Crawford (1997), Identifying and removing barometric pressure effects in confined and unconfined aquifers, *Ground Water*, *35*, 502–511.

Rutledge, A. T. (1993), Computer programs for describing the recession of ground-water discharge and for estimating mean ground-water recharge and discharge from streamflow records, *U.S. Geol. Surv. Water Resour. Invest. Rep.*, *93-4121*, 45 pp., US Geol. Surv., Denver, Colo.

Saar, M. O., M. C. Castro, C. M. Hall, M. Manga, and T. P. Rose (2005), Quantifying magmatic, crustal, and atmospheric helium contributions to volcanic aquifers using all stable noble gases: Implications for magmatism and groundwater flow, *Geochem. Geophys. Geosyst.*, *6*, Q03008, doi:10.1029/2004GC000828.

Schlosser, P., M. Stute, C. Sonntag, and K. O. Munnich (1989), Tritiogenic ^{3}He in shallow groundwater, *Earth Planet. Sci. Lett.*, *94*, 245–256.

Stute, M., and J. Deak (1989), Environmental isotope study (^{14}C, ^{13}C, ^{18}O, D, noble gases) on deep groundwater circulation systems in Hungary with reference to paleoclimate, *Radiocarbon*, *31*(3), 902–918.

Stute, M., and P. Schlosser (1993), Principles and applications of the noble gas paleothermometer, in *Climate Change in Continental Isotopic Records, Geophys. Monogr. Ser.*, edited by P. K. Smart et al., vol. 78, pp. 89–100, AGU, Washington, D. C.

Stute, M., P. Schlosser, J. F. Clark, and W. S. Broecker (1992), Paleotemperatures in the southwestern United States derived from noble gases in ground water, *Science*, *256*(5059), 1000–1001.

Stute, M., M. Forster, H. Frischkorn, A. Serjo, J. F. Clark, P. Schlosser, W. S. Broecker, and G. Bonani (1995), Cooling of tropical Brazil (5°C) during The Last Glacial Maximum, *Science*, *269*(5222), 379–383.

Sun, T., C. M. Hall, M. C. Castro, K. C. Lohmann, and P. Goblet (2008), Excess air in the noble gas groundwater paleothermometer: A new model based on diffusion in the gas phase, *Geophys. Res. Lett.*, *35*, L19401, doi:10.1029/2008GL035018.

Sun, T., C. M. Hall, and M. C. Castro (2010), Statistical properties of groundwater noble gas paleoclimate models: Are they robust and unbiased estimators?, *Geochem. Geophys. Geosyst.*, *11*, Q02002, doi:10.1029/2009GC002717.

Toll, N. J., and T. C. Rasmussen (2007), Removal of barometric pressure effects and Earth tides from observed water levels, *Ground Water*, *45*(1), 101–105.

Van Camp, M., and P. Vauterin (2005), TSOFT: Graphical and interactive software for the analysis of time series and Earth tides, *Comput. Geosci.*, *31*(5) 631–640.

M. C. Castro, C. M. Hall, and K. C. Lohmann, Department of Earth and Environmental Sciences, University of Michigan, Ann Arbor, MI 48109-1005, USA. (cmhall@umich.edu)

T. Sun, Center for Petroleum and Geosystems Engineering, Cockrell School of Engineering, University of Texas at Austin, 1 University Station C0304, Austin, TX 78712, USA.